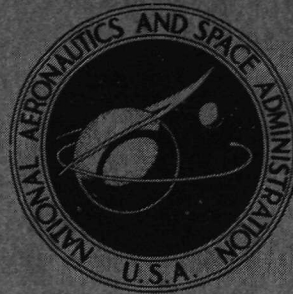


N72-14027

NASA TECHNICAL
MEMORANDUM



NASA TM X-2480

NASA TM X-2480

CASE FILE
COPY

COMPUTER-CONTROLLED PERFORMANCE MAPPING
OF THERMIONIC CONVERTERS: EFFECT OF
COLLECTOR, GUARD-RING POTENTIAL
IMBALANCES ON THE OBSERVED COLLECTOR
CURRENT-DENSITY, VOLTAGE CHARACTERISTICS
AND LIMITED RANGE PERFORMANCE MAP OF AN
ETCHED-RHENIUM, NIOBIUM PLANAR CONVERTER .

by Eugene J. Manista

Lewis Research Center

Cleveland, Ohio 44135

NATIONAL AERONAUTICS AND SPACE ADMINISTRATION • WASHINGTON, D. C. • JANUARY 1972

1. Report No. NASA TM X-2480		2. Government Accession No.		3. Recipient's Catalog No.	
4. Title and Subtitle COMPUTER-CONTROLLED PERFORMANCE MAPPING OF THERMIONIC CONVERTERS: EFFECT OF COLLECTOR, GUARD-RING POTENTIAL IMBALANCES ON THE OBSERVED COLLECTOR CURRENT-DENSITY, VOLTAGE CHARACTERISTICS AND LIMITED RANGE PERFORMANCE MAP OF AN ETCHED-RHENIUM, NIOBIUM PLANAR CONVERTER				5. Report Date January 1972	
				6. Performing Organization Code	
7. Author(s) Eugene J. Manista				8. Performing Organization Report No. E-6446	
9. Performing Organization Name and Address Lewis Research Center National Aeronautics and Space Administration Cleveland, Ohio 44135				10. Work Unit No. 112-27	
				11. Contract or Grant No.	
12. Sponsoring Agency Name and Address National Aeronautics and Space Administration Washington, D. C. 20546				13. Type of Report and Period Covered Technical Memorandum	
				14. Sponsoring Agency Code	
15. Supplementary Notes					
16. Abstract <p>The effect of collector, guard-ring potential imbalance on the observed collector-current-density J, collector-to-emitter voltage V characteristic was evaluated in a planar, fixed-space, guard-ringed thermionic converter. The J, V characteristic was swept in a period of 15 msec by a variable load. A computerized data acquisition system recorded test parameters. The results indicate minimal distortion of the J, V curve in the power output quadrant for the nominal guard-ring circuit configuration. Considerable distortion, along with a lowering of the ignited-mode striking voltage, was observed for the configuration with the emitter shorted to the guard ring. A limited-range performance map of an etched-rhenium, niobium, planar converter was obtained by using an improved computer program for the data acquisition system. The new program accumulates J, V data at predefined emitter, collector, and cesium-reservoir, temperatures T_E, T_C, and T_R by controlling the application of the variable load while continuously monitoring T_E, T_C, and T_R. Current, voltage data were taken at 50 K increments in T_E and T_C for $1750 \text{ K} \leq T_E \leq 1900 \text{ K}$ and for $800 \text{ K} \leq T_C \leq 1000 \text{ K}$. Current-density, voltage envelopes for constant T_E or T_E and T_C are given.</p>					
17. Key Words (Suggested by Author(s)) Thermionic conversion Computer data acquisition				18. Distribution Statement Unclassified - unlimited	
19. Security Classif. (of this report) Unclassified		20. Security Classif. (of this page) Unclassified		21. No. of Pages 15	
				22. Price* \$3.00	

* For sale by the National Technical Information Service, Springfield, Virginia 22151

COMPUTER-CONTROLLED PERFORMANCE MAPPING OF THERMIONIC CONVERTERS:
EFFECT OF COLLECTOR, GUARD-RING POTENTIAL IMBALANCES ON THE OBSERVED
COLLECTOR CURRENT-DENSITY, VOLTAGE CHARACTERISTICS AND
LIMITED RANGE PERFORMANCE MAP OF AN ETCHED-RHENIUM,
NIOBIUM PLANAR CONVERTER

by Eugene J. Manista
Lewis Research Center

SUMMARY

The effect of collector, guard-ring potential imbalance on the observed collector-current-density J , collector-to-emitter voltage V characteristic was evaluated in a planar, fixed-space, guard-ringed thermionic converter. The J, V characteristic was swept in a period of 15 milliseconds by a variable load. A computerized data acquisition system recorded test parameters. The results indicate minimal distortion of the J, V curve in the power output quadrant for the nominal guard-ring circuit configuration. Considerable distortion, along with a lowering of the ignited-mode striking voltage, was observed for the configuration with the emitter shorted to the guard ring.

A limited-range performance map of an etched-rhenium, niobium planar converter was obtained by using an improved computer program for the data acquisition system. The new program accumulates J, V data at predefined emitter, collector, and cesium-reservoir temperatures T_E , T_C , and T_R by controlling the application of the variable load while continuously monitoring T_E , T_C , and T_R . Current, voltage data were taken at 50 K increments in T_E and T_C for $1750 \text{ K} \leq T_E \leq 1900 \text{ K}$ and for $800 \text{ K} \leq T_C \leq 1000 \text{ K}$. Current-density, voltage envelopes for constant T_E or T_E and T_C are given.

INTRODUCTION

More power at lower temperatures is the goal for nuclear thermionic diodes. Providing that improvement means intensive testing of the best existing emitters and col-

lectors, promising new electrodes, and additives. To ensure success, performance mapping must cover off-design as well as optimum operating conditions - with special attention to stability problems. Enormous quantities of current, voltage data are inevitable in these detailed performance studies. For example, approximately 500 current, voltage curves at selected emitter, collector, and cesium reservoir temperatures are needed to define the emission and collection properties of just a single combination of electrode materials.

A computer-controlled thermionic data system has been developed (ref. 1) to acquire and process these performance data. The system not only reduces the experimental burden and time required to obtain the data but also organizes the large mass of data for subsequent analysis and display (ref. 2).

This report presents the results of a series of tests to assess the effects of collector, guard-ring potential imbalance and test circuit conditions on the current, voltage characteristics observed with the data system. A new data recording and experimental sequence control program is described, and its use is illustrated by a remap of a fixed-spacing etched-rhenium, niobium converter over a limited range of conditions. Results of the performance remap are given and compared with those obtained earlier (ref. 2).

EFFECT OF COLLECTOR, GUARD-RING POTENTIAL IMBALANCE ON THE OBSERVED CURRENT, VOLTAGE CHARACTERISTIC

Several experimental effects can confuse the interpretation of the collector current, voltage properties of a cesiated converter. Particularly troublesome in planar converters are the spurious emission currents arising from the emitter edges and the walls of the enclosure. These currents can often be significantly reduced by the incorporation of an active guard ring around the collector electrode. If the surface potential and temperature of the guard ring can be maintained close to those of the collector during the data observing period, this electrode will collect these currents and also tend to eliminate internal leakage from the emitter to the collector. Employed in this manner, the guard ring serves the highly important function of defining the collection area of the converter. Performance data of combinations of electrode materials from different converter structures can then be readily compared.

Balancing the guard-ring potential closely to that of the collector, either electronically or manually, slows down the rate of performance data accumulation tremendously. As the guard ring seeks collector potential balance during a slowly varying converter loading, the emitter and collector surface temperatures T_E and T_C tend to drift because of the accompanying changes in the heat fluxes to and from these surfaces. Such drifts in T_E and T_C , if appreciable, can introduce larger deviations in the current,

voltage characteristic than those attributed to collector, guard-ring imbalance. In the extended-range performance mapping tests the thermal inertia present in the emitter and collector electrode structures of the converter is utilized to minimize the effects of temperature drift during the current, voltage observing period. This is accomplished by biasing the converter to a low-current, retarded-voltage condition while setting the desired emitter, collector, and cesium-reservoir temperatures. A varying load is then imposed to obtain the full characteristic. The load variation is about 15 milliseconds in duration and sweeps the output from the retarded condition to a forward bias of a few volts and back to the retarded condition. During the loading, a computer-controlled multiplexer and analog-to-digital converter samples and stores 90 current, voltage points.

The nominal test circuit used and the signal sources are shown in figure 1. Careful placement of the current sensing leads and the use of low-inductance shunts are required to measure the collector current with this technique since rates of change of the converter current often exceed 10^4 amperes per second and inductive distortion of the curve can occur. Improper shunt selection and insufficient amplifier bandwidth cause hysteresis in the observed curve of current-density J plotted against voltage V , particularly along the rapidly changing current segments of the characteristic. To reduce the relative effect, the resistance of the collector shunt can be increased and the channel gain decreased; however, this causes increased potential imbalance between the collector and guard ring, which may distort the characteristic more than the original inductive effect.

Hysteresis in the J, V curve can also develop from other sources. Among these are variations in the surface temperatures of the emitter and collector, changes in the cesium arrival rate at the electrode surfaces, and observations of the J, V characteristic in a time interval comparable to the intrinsic relaxation processes governing the emission, collection, and transport of the electron and ionic currents of the device.

To provide an estimate of the distortion that can arise, the influence of different guard-ring circuit conditions on the observed J, V curve was evaluated in a planar, fixed-spacing converter. The converter design is described in reference 3.

Current, voltage data were taken at three external guard-ring circuit conditions: the nominal test circuit, wherein guard-ring current is allowed to flow, but is not measured; an open circuit condition wherein the guard-ring electrode is allowed to float; and an externally shorted condition wherein guard-ring current is shunted directly to the emitter. The influence of different combinations of the collector shunt and the amplifier gain was also evaluated for the nominal guard-ring configuration. Collector current, collector-to-emitter voltage, and guard-ring-to-emitter voltage were recorded by using the data acquisition system program of reference 1.

Guard-Ring Circuit Condition Results

Results of the guard-ring circuit condition tests are shown in figure 2. The J, V curve obtained with the nominal configuration is plotted as the circles, the curve obtained at the open-circuit condition is shown as the dashed line, and the curve obtained at short circuit is shown as the continuous line. All collector currents were measured with a 0.01-ohm shunt and an amplifier gain of 50 to keep the shunt drop below 200 millivolts. The J, V curve in the power quadrant is significantly influenced by the imposition of the extreme guard-ring potential conditions. In particular, as the collector electrode is driven position relative to the emitter, deviations from the J, V curve taken with the nominal configuration and the J, V curves taken with the extreme guard-ring conditions become appreciable. A significant alteration of the J, V curve occurs for the short-circuited case; the striking potential necessary to pass from the passive mode to the ignited mode is lowered. The ease of transition to the ignited mode branch is attributed to ion current flow from the guard-ring, emitter discharge volume into the emitter, collector volume. In figure 3, the guard-ring-to-emitter voltage is plotted against the collector-to-emitter voltage for the corresponding conditions. The guard-ring potential is seen to follow the collector potential quite closely over the entire range for the nominal configuration. In the case of the shorted guard-ring condition, the guard-ring, emitter space is in an ignited mode, as can be inferred from the constant value of the guard-ring-to-emitter voltage. And as the collector potential approaches and exceeds that of the guard-ring, emission current that would normally flow to the guard ring begins to be collected by the collector electrode. In the floating guard-ring case, the guard-ring, emitter space remains in the passive mode throughout the sweep, as indicated in figure 3. And as the collector-emitter space becomes ignited, emission current again starts to be collected by the collector electrode.

Shunt and Amplifier Gain Results

The effect of small guard-ring-to-collector potential imbalances on the J, V curve is shown in figure 4. Shunt and amplifier gain combinations used to measure the collector current were 0.01 ohm and 50 for the J, V points plotted as circles and 0.1 ohm and 10 for the J, V points plotted as triangles. With the latter combination, the guard-ring potential is slightly more positive than the collector potential at the same current density as in the former shunt and gain combination. The two curves agree quite well in magnitude and shape. Closer inspection reveals that the J, V curve obtained with the 0.1-ohm shunt differs by approximately 8 percent from that obtained with the 0.01-ohm shunt. A discrepancy of this amount is easily accountable by only a 10 K difference between the emitter temperatures at which the data were taken.

The hysteresis observed in the ignited mode branch of both curves is a real effect, characteristic of the time development of the ignited mode discharge at these emitter and cesium-reservoir temperatures. Comparing the two curves, one observes that the separation is less in the 0.1-ohm case than in the 0.01-ohm case. This is due to the unequal rates of loading imposed by the transistorized load circuit. From the relative spacing between the sampled data points, it can be inferred that the discharge was developed more slowly in the 0.1-ohm test than in the 0.01-ohm test. This hysteresis has been observed to diminish in magnitude as the cesium-reservoir temperature is increased.

LIMITED-RANGE PERFORMANCE MAP OF AN ETCHED-RHENIUM, NIOBIUM PLANAR CONVERTER

The thermionic properties of an etched-rhenium emitter and niobium collector have been mapped in detail in reference 2 by using the J, V data acquisition system program of reference 1. Since the new J, V data acquisition system and the experimental sequencing program are considerably different from the original system, the thermionic performance of this converter was remapped over a limited range of emitter temperatures to verify that the results obtained by using the partially automated system agreed with those obtained earlier.

New Thermionic Data Recording Program

A new data recording program has been written with several features which reduce the experimental burden involved in gathering large quantities of performance data. A block diagram of the logical flow is given in figure 5. Before placing a call to record test data, the experimenter enters input data associated with the converter and the test into three tables in memory. This information is used by the data recording program for indexing, control, and data reduction of the temperature sensors. A standard teletype is used for this data transfer.

Performance data from fixed-spacing converters of the design given in reference 3 are obtained by slowly ramping the emitter temperature at constant collector and cesium-reservoir temperatures. A data record call to the system initiates the program. After coupling the data input lines to the bank of 16 differential amplifiers for analog signal conditioning, the program, following a 5-second delay, checks T_R to see that it is near the level requested by the programmed Go/No value. If T_R is within bounds (typically set to within ± 2 K), the system then continuously samples the T_E data channel

until the value is equal to (within ± 8 K of) that requested for the first sweep (the Temperature level data table values). Upon reaching this condition, the system triggers the variable load.

The J, V characteristic of the converter is swept from a low-current, retarding condition to a forward bias of a few volts and back to the retarded condition in about 15 milliseconds. During the load variation the J, V characteristic is sampled 90 times with sample-and-hold amplifiers to coordinate in time the collector current and the collector-to-emitter potential difference.

The system tests for the end of the load variation before reading in T_E , T_C , and T_R , and bookkeeping information that provides absolute scaling of the current and voltage and identification data to aid in subsequent data processing schemes. Between J, V sweeps the temperature data are processed to Kelvin.

Up to six different T_E 's can be introduced as input data. The thermal time constants of the converter and of the collector and cesium-reservoir temperature controllers limit the range and rapidity of the emitter temperature ramp to about 250 K over a 20-second interval. With this limit on emitter temperature variation the observed collector temperature is within ± 10 K of the desired value for all six sweeps.

Instrumentation

The collector current developed in the converter was measured from the potential drop across either a 0.01- or 0.1-ohm shunt by using the nominal guard-ring circuit configuration. Collector-to-emitter potential difference was measured at the external shroud of the converter. No corrections were made for the voltage drop in the emitter support since it is small in this converter design.

As in the test program of reference 2, the collector and the cesium-reservoir temperatures were observed with sheathed Chromel-Alumel thermocouples. The same thermocouples were used to eliminate the introduction of a possible systematic error.

The emitter temperature, however, was measured by a different pyrometric instrument. An automatic brightness temperature pyrometer, focused onto the black-body cavity in the edge of the emitter (cavity length-to-diameter ratio of 5), provided the signal source for the emitter temperature measurement. The optical path (the dominant element being the vacuum sighting window) and the pyrometer were calibrated against an NBS-certified tungsten-strip lamp. The response time of the pyrometer for a 100 K step change in source temperature was about 1 second to reach 99 percent of the final reading. An uncertainty of ± 10 K was associated with the emitter temperature measuring system. Observed temperatures were not corrected for temperature gradients to the active emitting surface since these corrections were small, about -11 K at 1750 K to

about -16 K at 1900 K according to the one-dimensional heat-transfer model suggested in reference 2.

Test Sequence

The converter was mapped by fixing T_R and T_C and then ramping T_E , either upwards or downwards by changing the input power to the emitter. Data were obtained at emitter temperatures of 1750, 1800, 1850, and 1900 K. The collector temperature was then changed by 50 K to obtain T_C values from 800 to 1000 K, and the T_E ramp was repeated at constant T_R . A new value of T_R was then established, and the T_E , T_C variation repeated. Five T_R values between 560 and 640 K, spaced 20 K apart, were established.

PERFORMANCE MAPPING RESULTS

Data Processing

The set of performance data is transferred to a magnetic tape file at the local central computing center. During transfer the current and voltage are converted to absolute engineering units and the power density points are calculated. Further computer processing sorts and arranges the data into groups of constant T_E , constant T_C , and increasing levels of T_R .

Another computer processing step scales and prepares a data input tape which is used to present the J, V curves in graphical form on an oscilloscope, 35-millimeter-camera plotting system. The plotting routine rejects current-density data that correspond to saturated analog amplifier levels and fixes the output axes at -0.50 to 2.00 volts and 0 to 30 amperes per square centimeter. The J, V data are plotted individually and in groups with T_E , T_C , and T_C , or T_E and T_R constant.

Data Presentation

The fully developed J, V envelopes for the etched-rhenium, niobium system at 1750, 1800, 1850, and 1900 K are shown in figure 6 as the solid curves; the earlier results obtained for this converter (ref. 2) are shown as the dashed curves. Excellent agreement is seen for all curves except for the slight variation found in the 1750 K curve.

Figures 7 to 10 present the envelopes at constant T_E and T_C and illustrate the performance variation found as a function of collector temperature. In these presentations, different values of T_R contribute points to the J, V envelope curves. Cesium-reservoir levels near 640 K contribute data only to the higher current-density points. In the region of interest to practical thermionic module design, 12 to 18 amperes per square centimeter, a cesium-reservoir temperature of 600 to 620 K would be required.

CONCLUDING REMARKS

Extreme guard-ring, collector potential imbalance was observed to seriously distort the current, voltage characteristic of a planar converter. The nominal test circuit configuration, in which the guard-ring potential is maintained close to (within 200 mV of) that of the collector, yields reproducible current, voltage curves.

A new data recording and experimental sequence control program which automatically accumulates performance data at prescribed emitter and cesium reservoir temperatures was described. Constant emitter temperature envelopes of an etched-rhenium, niobium planar converter were obtained by using the new program. The envelopes were in good agreement with those which had been observed from data gathered by the original data acquisition system-program.

Lewis Research Center,
National Aeronautics and Space Administration,
Cleveland, Ohio, October 21, 1971,
112-27.

REFERENCES

1. Breitwieser, R.; Manista, E. J.; and Smith, A. L.: Computerized Performance Mapping of a Thermionic Converter with Oriented Tungsten Electrodes. Proceedings of the Thermionic Conversion Specialist Conference. IEEE, 1969, pp. 90-99.
2. Lancashire, Richard B.: Computer-Acquired Performance Map of an Etched-Rhenium, Niobium Planar Diode. Proceedings of the Thermionic Conversion Specialist Conference. IEEE, 1970, pp. 487-491.
3. Speidel, T. O.; and Williams, R. M.: Fixed-Space Planar Thermionic Diode with Collector Guard Ring. Proceedings of the Thermionic Conversion Specialist Conference. IEEE, 1968, pp. 113-117.

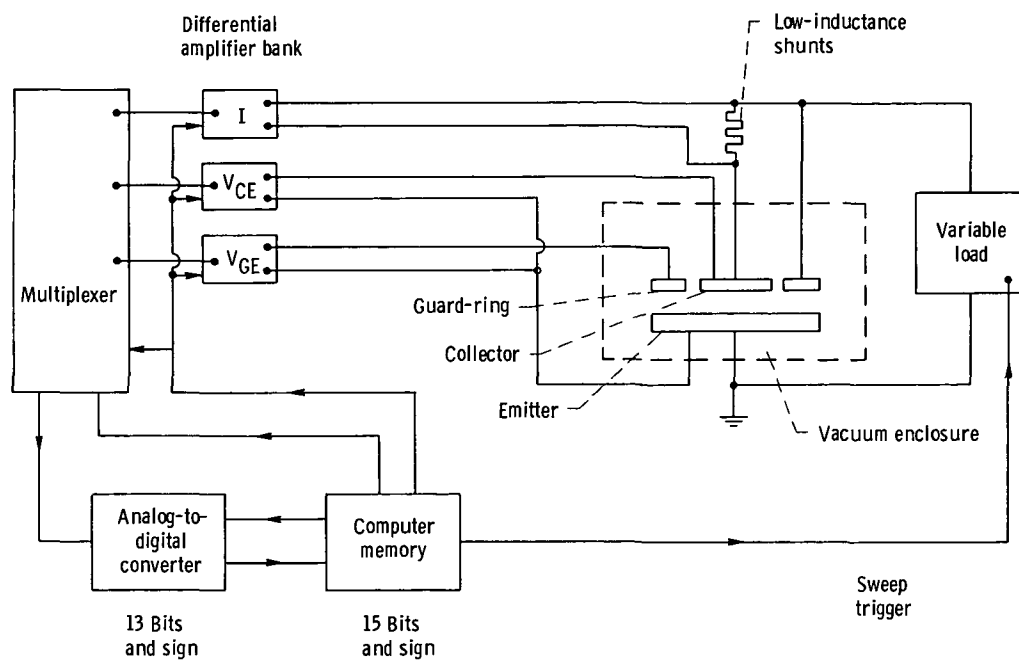


Figure 1. - Nominal test circuit configuration for performance mapping of thermionic converters.

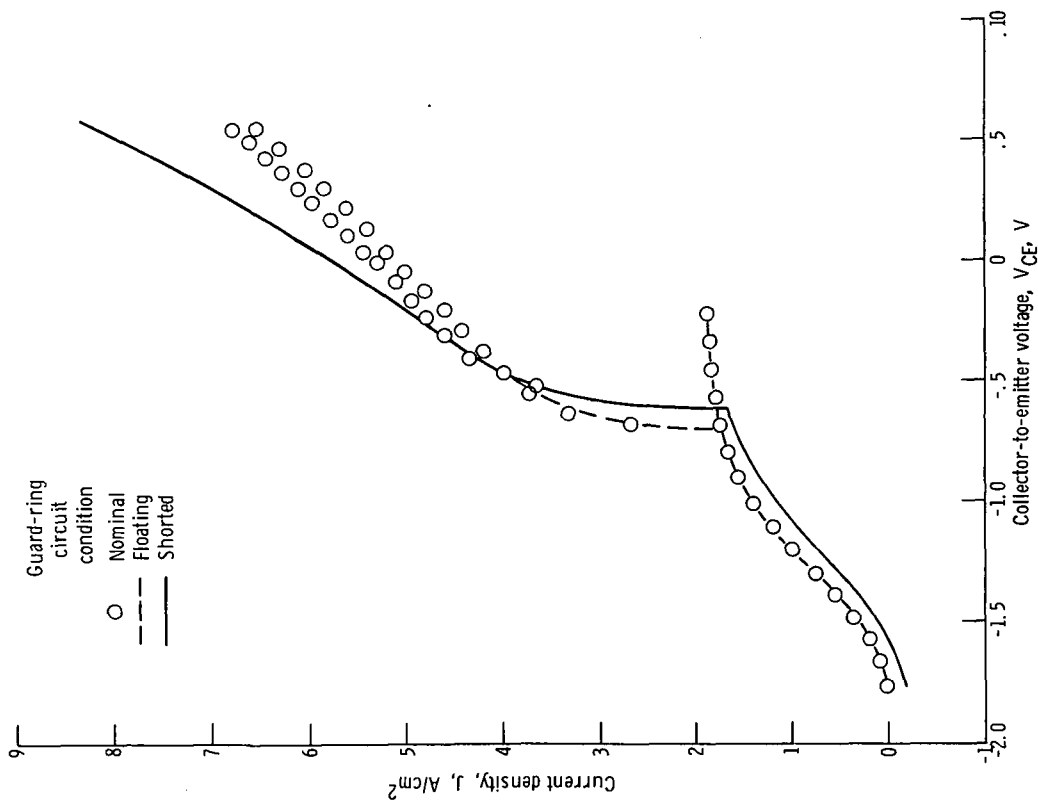


Figure 2. - Collector current density as function of collector-to-emitter voltage for different guard-ring circuit conditions. Emitter temperature, 1800 K; collector temperature, 856 K; cesium-reservoir temperature, 565 K; interelectrode spacing, 0.25 millimeter.

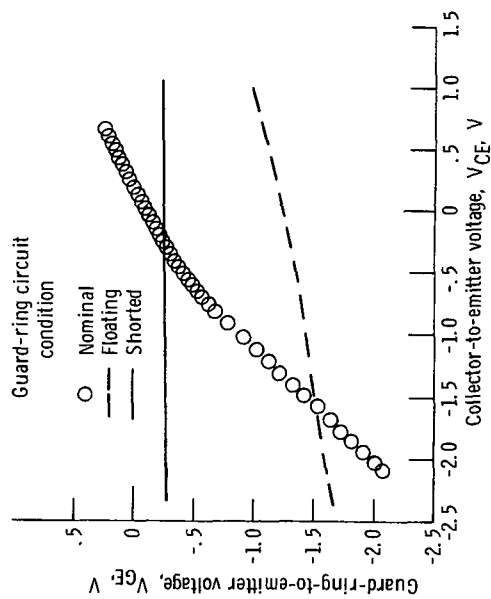


Figure 3. - Guard-ring-to-emitter voltage as function of collector-to-emitter voltage for three guard-ring circuit conditions. Emitter, etched rhenium; collector, niobium; emitter temperature, 1800 K; collector temperature, 856 K; cesium-reservoir temperature, 565 K; interelectrode spacing, 0.25 millimeter.

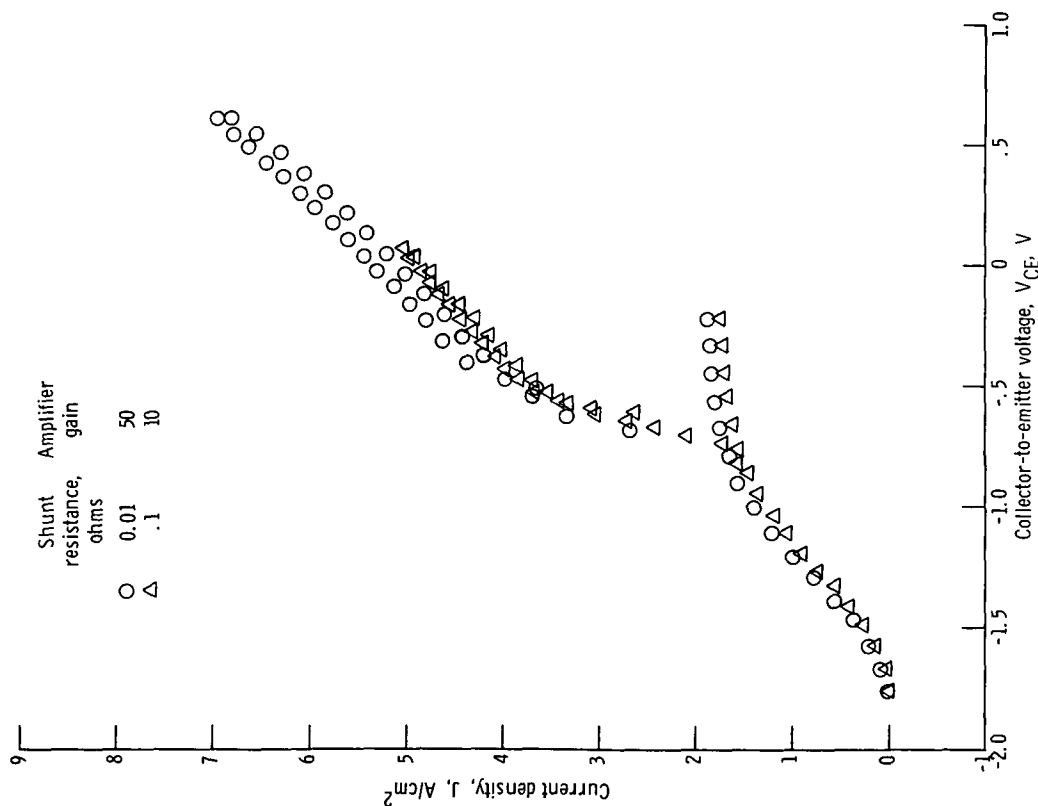


Figure 4. - Collector current density as function of collector-to-emitter voltage for different shunt and amplifier gain combinations. Emitter temperature, 1800 K; collector temperature, 856 K; cesium-reservoir temperature, 565 K; interelectrode spacing, 0.25 millimeter.

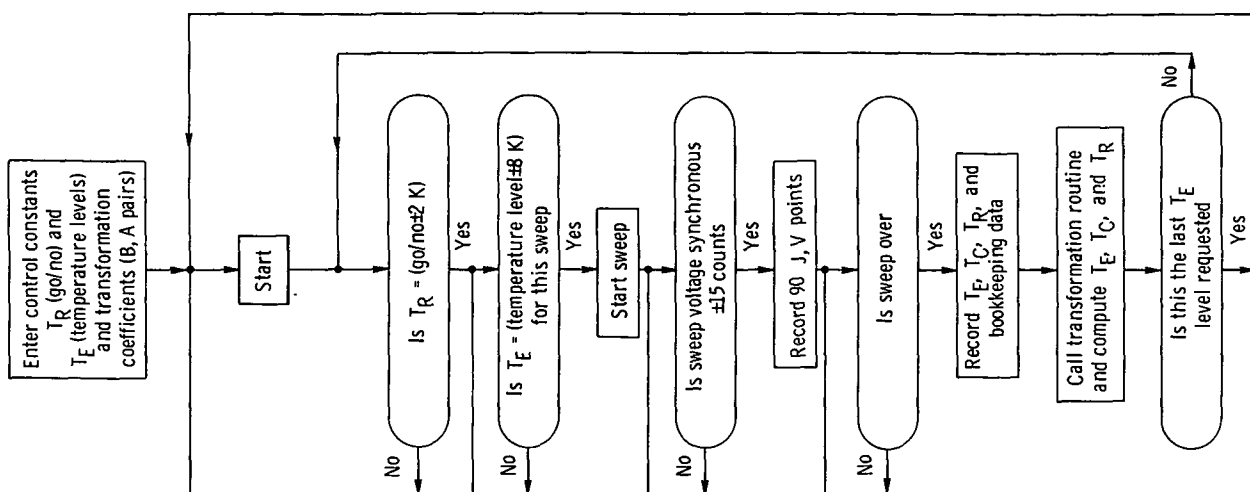


Figure 5. - New experimental control program for fixed-space current-density, voltage data acquisition.

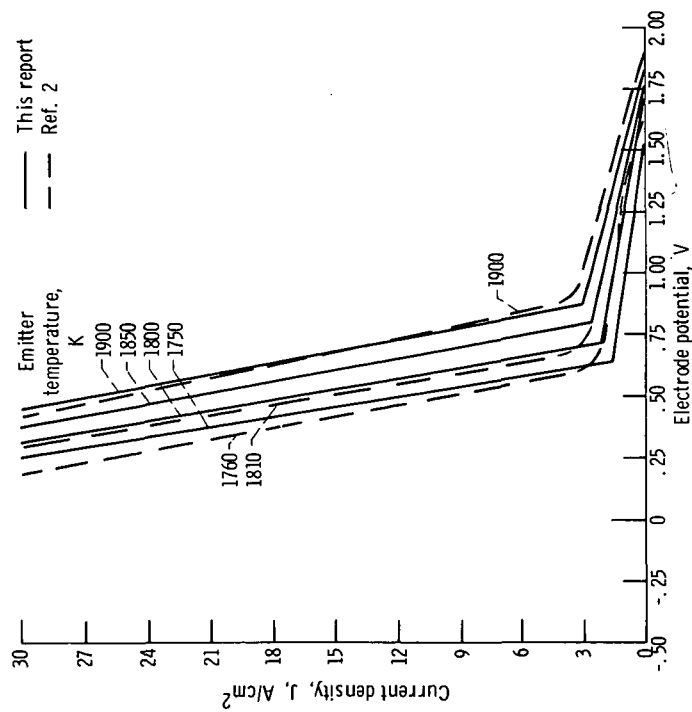


Figure 6. - Performance envelopes for etched-rhenium, niobium converter at various emitter temperatures.

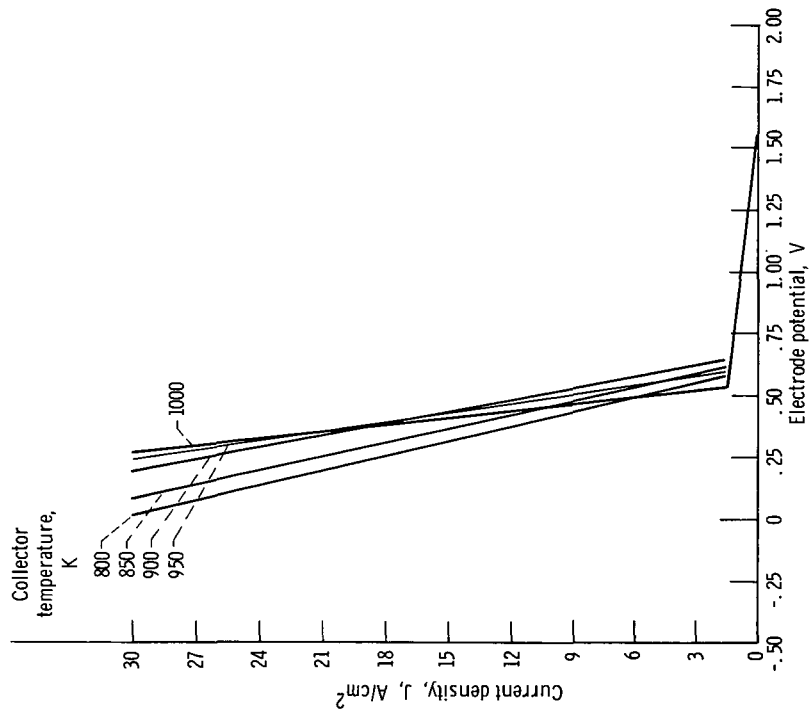


Figure 7. - Constant emitter temperature envelopes for etched-rhenium, niobium planar converter at various collector temperatures. Emitter temperature, 1750 K.

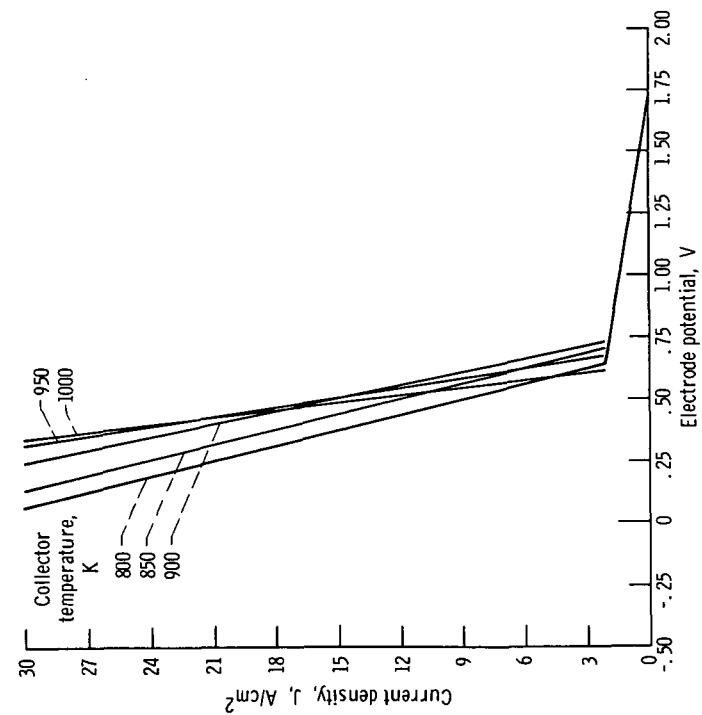


Figure 8. - Constant emitter temperature envelopes for etched-rhenium, niobium planar converter at various collector temperatures. Emitter temperature, 1800 K.

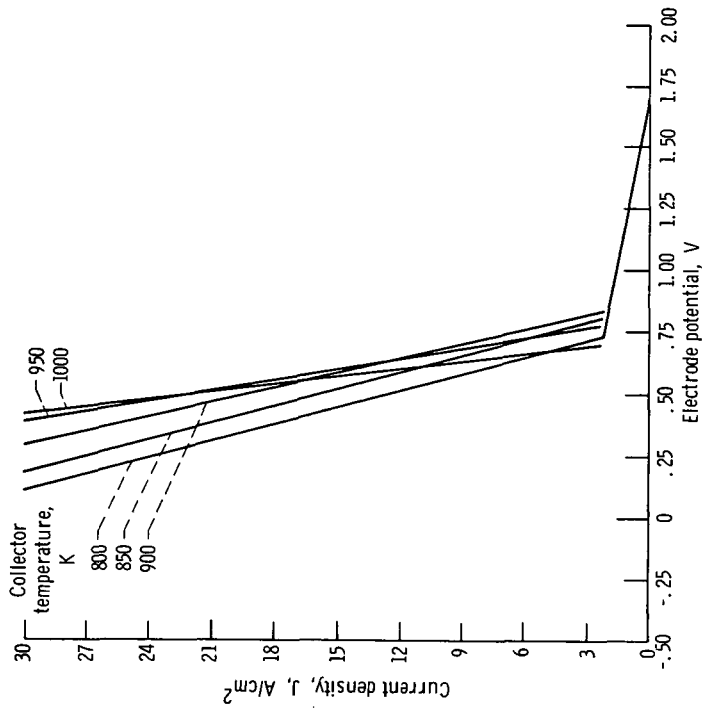


Figure 9. - Constant emitter temperature envelopes for etched-rhenium, niobium planar converter at various collector temperatures. Emitter temperature, 1850 K.

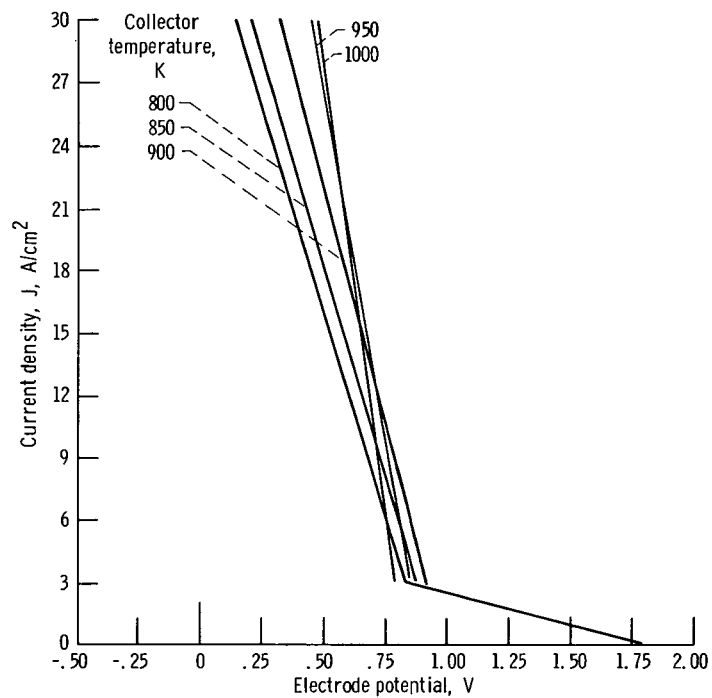


Figure 10. - Constant emitter temperature envelopes for etched-rhenium, niobium planar converter at various collector temperatures. Emitter temperature, 1900 K.

NATIONAL AERONAUTICS AND SPACE ADMINISTRATION
WASHINGTON, D.C. 20546

OFFICIAL BUSINESS
PENALTY FOR PRIVATE USE \$300

FIRST CLASS MAIL

POSTAGE AND FEES PAID
NATIONAL AERONAUTICS AND
SPACE ADMINISTRATION



POSTMASTER: If Undeliverable (Section 158
Postal Manual) Do Not Return

"The aeronautical and space activities of the United States shall be conducted so as to contribute . . . to the expansion of human knowledge of phenomena in the atmosphere and space. The Administration shall provide for the widest practicable and appropriate dissemination of information concerning its activities and the results thereof."

— NATIONAL AERONAUTICS AND SPACE ACT OF 1958

NASA SCIENTIFIC AND TECHNICAL PUBLICATIONS

TECHNICAL REPORTS: Scientific and technical information considered important, complete, and a lasting contribution to existing knowledge.

TECHNICAL NOTES: Information less broad in scope but nevertheless of importance as a contribution to existing knowledge.

TECHNICAL MEMORANDUMS: Information receiving limited distribution because of preliminary data, security classification, or other reasons.

CONTRACTOR REPORTS: Scientific and technical information generated under a NASA contract or grant and considered an important contribution to existing knowledge.

TECHNICAL TRANSLATIONS: Information published in a foreign language considered to merit NASA distribution in English.

SPECIAL PUBLICATIONS: Information derived from or of value to NASA activities. Publications include conference proceedings, monographs, data compilations, handbooks, sourcebooks, and special bibliographies.

TECHNOLOGY UTILIZATION PUBLICATIONS: Information on technology used by NASA that may be of particular interest in commercial and other non-aerospace applications. Publications include Tech Briefs, Technology Utilization Reports and Technology Surveys.

Details on the availability of these publications may be obtained from:

**SCIENTIFIC AND TECHNICAL INFORMATION OFFICE
NATIONAL AERONAUTICS AND SPACE ADMINISTRATION
Washington, D.C. 20546**